Model Accuracy Assessment in Reaction-Diffusion Pattern Formation in Wireless Sensor Networks

Thomas C. Henderson, Anshul Joshi, Kirril Rashkeev, and Narong Boonsirisumpun
University of Utah

Kyle Luthy and Edward Grant
North Carolina State University

UUCS-13-003

School of Computing
University of Utah
Salt Lake City, UT 84112 USA

30 May 2013

Abstract

We propose to exploit reaction-diffusion (RD) patterns as part of the wireless sensor network (*S-Net*) high-level structure building toolkit; e.g., to support leader selection or to provide pathways through the network. In particular, we study the formation of RD spot and stripe patterns in *S-Nets* for which no coördinate frame exists; i.e., the nets have only topological connectivity determined by the inter-node broadcast range. We further demonstrate how macro-features of the RD patterns can be used for Bayesian model accuracy assessment of the difference between a uniform grid layout of the nodes versus an irregular grid due to error in node placement.

1 Introduction

Alan Turing introduced a revolutionary reaction-diffusion model as the chemical basis of morphogenesis [35], and this method lends itself particularly well to pattern synthesis in distributed systems. For more detailed explanations, see his original paper (which provides an exemplar of the scientific paper – theory, analysis and numerical solution on the Manchester machine which Turing helped design and build!), as well as the works of Murray [25], Meinhardt [23], and more recently, Maini and Othmer [22]. Turing's key insight was that diffusion of an inhibitory morphogen could lead to the formation of stable and variegated patterns. This is related to nonlinear far from equilibrium thermodynamics, and dissipative structures (e.g., see Prigogine [27, 30, 31] who received the Nobel prize in chemistry for work in this area). One goal of our work is to understand how these principles may be exploited in *S-Nets*.

We have previously proposed to use Turing's reaction-diffusion mechanism to generate patterns in *S-Nets*. [10, 15]. The basis of this mechanism is a set of equations that capture the reaction and diffusion aspects of certain chemical kinetics:

$$\frac{\partial \mathbf{c}}{\partial t} = f(\mathbf{c}) + D\nabla^2\mathbf{c} \tag{1}$$

where $f(\mathbf{c})$ describes the reaction and $D\nabla^2 c$ expresses the diffusion component. The simplest such systems have two *morphogens* or variables; one of these acts as the activator and the other acts as the inhibitor. The two variable system can be modeled by:

$$\frac{\partial u}{\partial t} = \gamma f(u,v) + \nabla^2 u, \frac{\partial v}{\partial t} = \gamma g(u,v) + d\nabla^2 v \tag{2}$$

where u and v are the concentrations of the morphogens, d is the diffusion coefficient and γ is a constant measure of scale. The functions $f(u,v)$ and $g(u,v)$ represent the reaction kinetics. As an example, we have explored the generation of spatial patterns using the Turing system of equations:

$$f(u,v) = \beta - uv, g(u,v) = uv - v - \alpha$$

where u and v are the morphogen concentrations, α and β are the decay and growth rates, respectively, and γ sets the speed of the reaction. They define a domain in which Equation (2) becomes linearly unstable to certain spatial disturbances. This domain is referred to as *Turing space* where the concentrations of the two morphogens will become unstable and result in the patterns shown in Figure 1. The pattern is the result of each cell running the equations locally while *diffusing* to its neighbors; a stable solution may be thresholded to produce a binary value at each sensor, and the total of these gives the pattern. Note that the distribution of these spots is close to hexagonal.

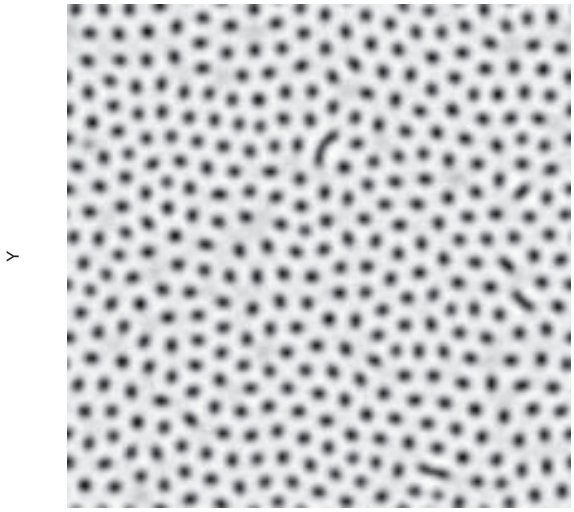

Figure 1: Turing Spot Pattern.

We introduced the use of Turing's reaction-diffusion pattern formation to support high-level tasks in *S-Nets*. This has led us to explore various biologically motivated mechanisms. We address below some issues that arise in trying to get reliable, efficient patterns in irregular grids. Others have explored the use of both reaction-diffusion and more general diffusion methods in computer vision and robotics. For example, Fukuda et al. describe the use of reaction-diffusion techniques in robot motion[7]. Moreover, as described by Peronna et al.[29], multi-scale descriptions of images (i.e., scale-space) can be produced by embedding the original image in a family of images obtained by convolving the original image with a filter; Koenderink[20] showed that this is equivalent to finding the solution of the diffusion equation:

$$I_t = \bigtriangledown^2 I = I_{xx} + I_{yy}$$

We believe that it will be quite useful for *S-Nets* to use similar methods to analyze sensed data of various sorts. Other proposed diffusion models include, for example, [16] who proposes directed diffusion - a datacentric communication coordination technique that "enables energy savings by selecting empirically good paths and by caching and processing data in- network." The focus of such work is more on the networking and operating systems aspects of the sensor network, whereas our work is more concerned with the sensor network as a computation engine itself. More closely related to our work is that of Justh and Krishnaprasad [17] who propose the active coordination of a large array of microactuators by means of diffusive coupling implemented as interconnection templates, and Nagpal [26] who describes methods to create patterns of diverse geometry. We believe that this style of research will reap great benefits in three aspects: (1) network *morphogenesis*, (2) sensed data analysis, and (3) display pattern synthesis.

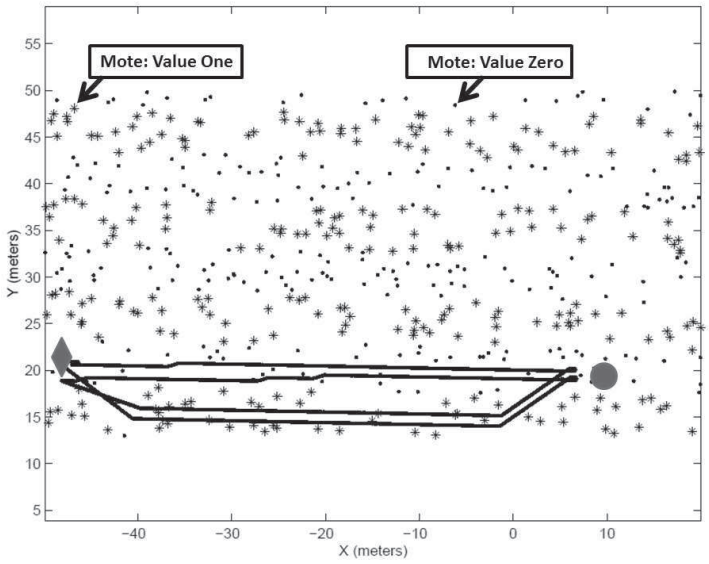

Figure 2: Robot Path in Reaction-Diffusion Pattern (○ is the fire control point; ◇ is the robot load point)

For example, consider a forest fire scenario: sensor devices are dropped into a wide geographic area, establish a network, and produce a stripe pattern of off-on signals that can be used by fire fighting agents to go to a fire control point by following *on* devices (pattern == 1) and return by following *off* devices (pattern == 0) (see Figure 2). Such patterns can be computed by very robust reaction-diffusion systems derived from models of biological pattern formation.

Our general research program is to explore a small set of biological sensing and signaling mechanisms, and we hope to make significant contributions by providing (1) biologically realistic models and efficient computational counterparts, (2) fault tolerant frameworks in which to run them, and (3) demonstrations of their application in human interface and large-scale sensor networks. In addition, we are building *S-Net* simulation, emulation, and experimentation testbeds [14]. Here we describe some initial results in the first of these areas.

Patterns in the *S-Net* can be used to support many high-level algorithms or activities:

- stripe, spot or ring patterns can be used as encoders for physical or logical purposes; for example, a robot can keep track of how far it has traveled (physical), or communication packets can travel along certain stripes to minimize power, cost or to avoid congestion (logical).

- certain sets of patterns form a basis set for 2D images (e.g., Haar or Hadamard basis sets); any map (topo, etc.) or image can then be encoded in terms of the coefficients associated with the respective basis images.
- the patterns can be used as a reference wave so that sensed data (or features derived from it) can be encoded as an interference pattern (i.e., a hologram)
- moving waves can also be computed, and thus the *S-Net* can serve as a signal carrier or modulator.

Understanding the precision and reliability of pattern formation is then of high importance.

Given a set of sensor elements, *SEL*s, in the plane, it may be useful to store and exploit a pattern in the *S-Net*. For example, stripes may be useful as described above (e.g., see [4, 13] for calculating shortest paths for robots to follow through terrain with varying traversability properties).

2 Reaction-Diffusion Patterns

Some work has already been done to determine the range and type of patterns possible with the Turing pattern formation approach. Theoretical aspects have been studied and regions of the parameter space characterized as they relate to pattern formation (i.e., the parameters are the coefficients in the PDEs) [2, 8, 21]. Others have investigated how pattern formation is influenced by number of cells, time scale, and initial condition variation. In particular, Bard and Lauder [3] showed that "stable repeating peaks of chemical concentration of periodicity 2-20 cells can be obtained in embryos in periods of time less than an hour. We do find however that these patterns are not reliable. Small variations in initial conditions give small but significant changes in the number and positions of observed peaks." They showed that this method has difficulty producing exact patterns reliably. We have found other difficulties in producing the patterns necessary to support higher-level tasks. We describe these here and propose some solutions.

A more significant issue for us is that the reaction-diffusion pattern formation equations assume that the inter-cell distance is uniform (and usually equal to 1). Our *S-Nets*, however, do not form a uniformly spaced grid in 1D or 2D nor do they have wrap-around connectivity; in fact, we generally assume that the sensor devices are randomly dropped in the environment. In addition, the diffusion part of the equations uses the inter-node distances in the computation of the second derivative. Two concerns are: (1) these distances are not

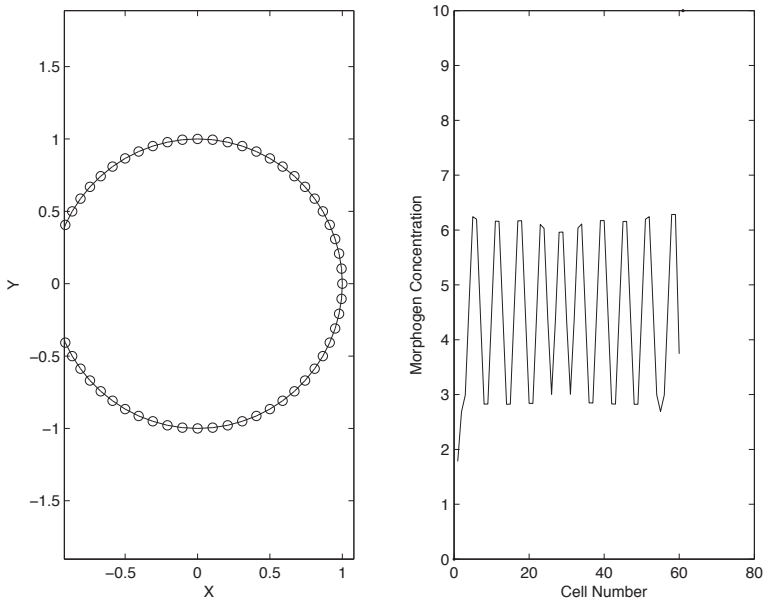

Figure 3: Typical 1-D Turing Pattern.

uniform, and (2) in an actual implementation, there will be some amount of error in the inter-node distance determination. This has led us to investigate the impact of non-uniform spacing on the pattern computation.

The basic 1D Turing reaction-diffusion mechanism on a ring of cells produces a pattern as shown in Figure 3 (the left side shows the ring layout of the cells and their connectivity; the right side shows the morphogen concentration in each cell after convergence), and takes about 1,040 iterations to converge for a set of 60 cells. The mean number of stripes (given random initial levels of morphogen b) is around 10.

Next consider what happens when error is introduced into the node locations, resulting in non-uniform distances between them. The point locations are determined as follows: (1) start with n points equi-spaced on the unit circle, $\frac{2*\pi}{n-1}$ units apart, and (2) add uniform noise to the location with max a angular (radians) distance from the uniform positions. Figure 4 shows the results of a uniformly sampled error from $\mathcal{U}(-5, 5)$ degrees, while Figure 5 shows what happens with a 10 degree uniformly sampled error. The graph shows the neighborhood relations formed by the radio broadcast range, and in the RD process, the *neighborhood Laplacian* is formed as:

$$\Delta a_i = (\sum_{n \in \mathcal{N}ei(i)} a_n) - |\mathcal{N}ei(i)|a_i$$

As can be seen, the change in the node neighborhood relations alters the macro feature

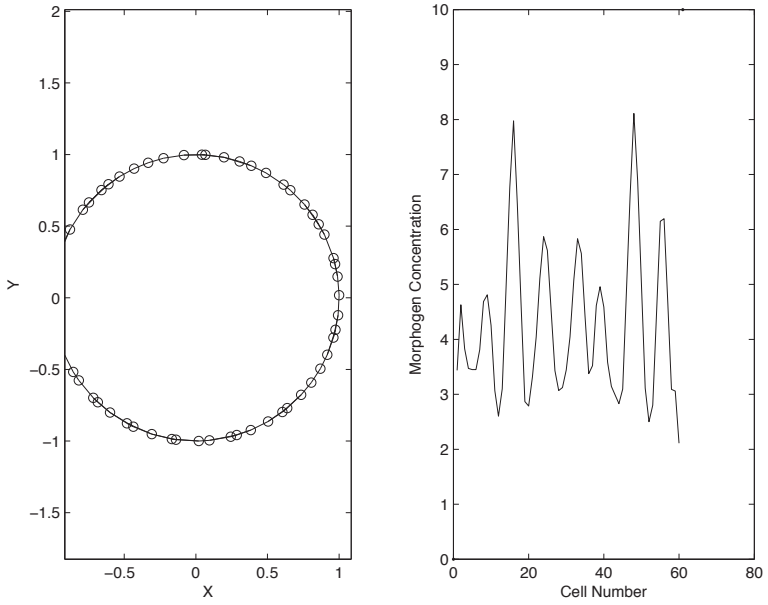

Figure 4: Turing Pattern Result for 5 Degree Error in Node Positions.

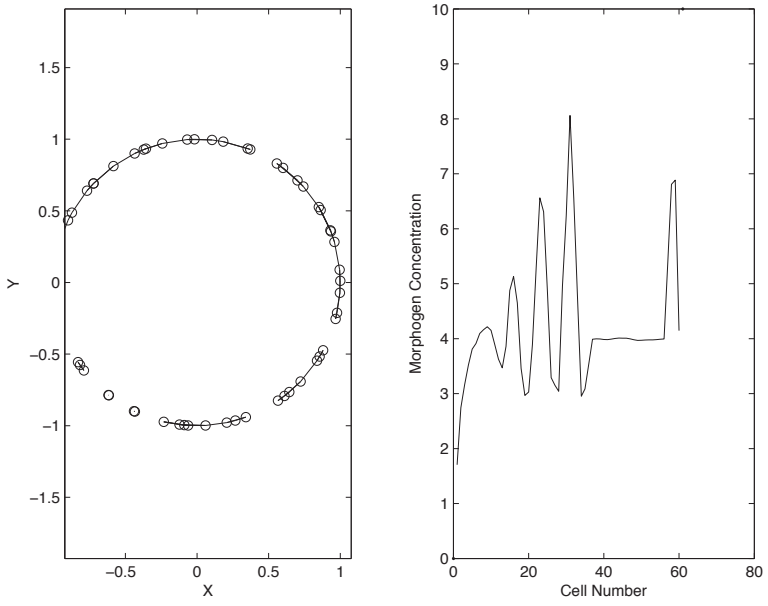

Figure 5: Turing Pattern Result for 10 Degree Error in Node Positions.

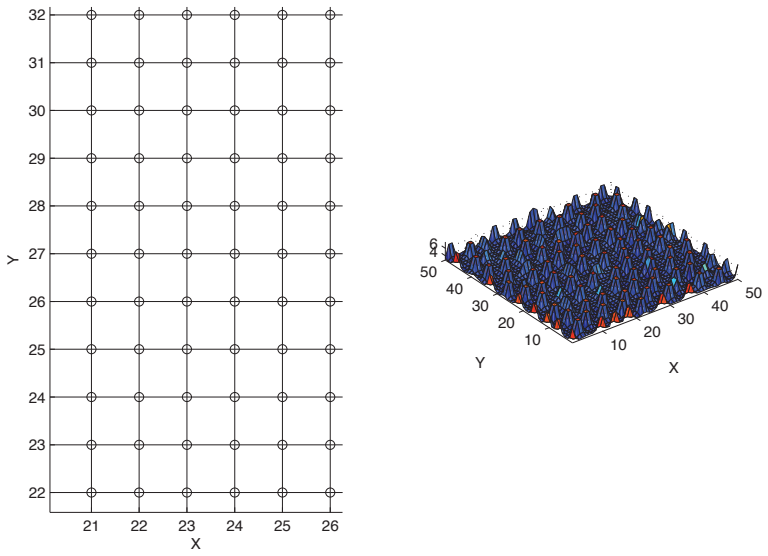

Figure 6: Turing Spot Pattern Result for 0 Error in Node Positions.

results; there are only eight stripes in the 5 degree error case, and four in the 10 degree error case, and the magnitudes of the peak concentrations vary significantly from the regular graph (cycle).

This result carries over into 2-D as well; Figures 6 through 8 show part of a displaced 50x50 grid (uniformly sampled error on $\mathcal{U}(0,0)$, $\mathcal{U}(-0.2,0.2)$, and $\mathcal{U}(-0.5,0.5)$ in x and y, respectively), and the resulting spots formed. As can be seen, the spots appear well-distributed and regular. Moreover, the neighborhood Laplacian works well. This is advantageous in *S-Nets* because inter-node distances are often hard to ascertain. Finally, note that the radio broadcast range of a node can vary between some min and max range (as a function of power), and this can change the network topology significantly; if neighborhoods extend over a larger area, then the spots will be larger in size (and fewer in number).

In order to form stripes in 2-D, Ermentrout [6] provides a coördinate-free RD mechanism for the creation of a stripe pattern. The equations are:

$$\frac{\partial u}{\partial t} = (a_{11} + \lambda)u - a_{21}v + Cu^3 + Qu^2 + d_1\Delta u$$

$$\frac{\partial v}{\partial t} = a_{12}u - a_{22}v + d_2\Delta v$$

where ∂t is approximated with $\delta t = 0.01$, $(a_{11} + \lambda) = 0.6$, $a_{21} = 1$, $a_{12} = 2$, $a_{22} + 4$, $d_1 = 0.08$, $d_2 = 1$, $C = 1$, and for $Q = 0$ stripes form (when $Q = 0.08$, spots form). The grid is intended to lie on a domain of 2πx2π, and thus δx is a function of the grid

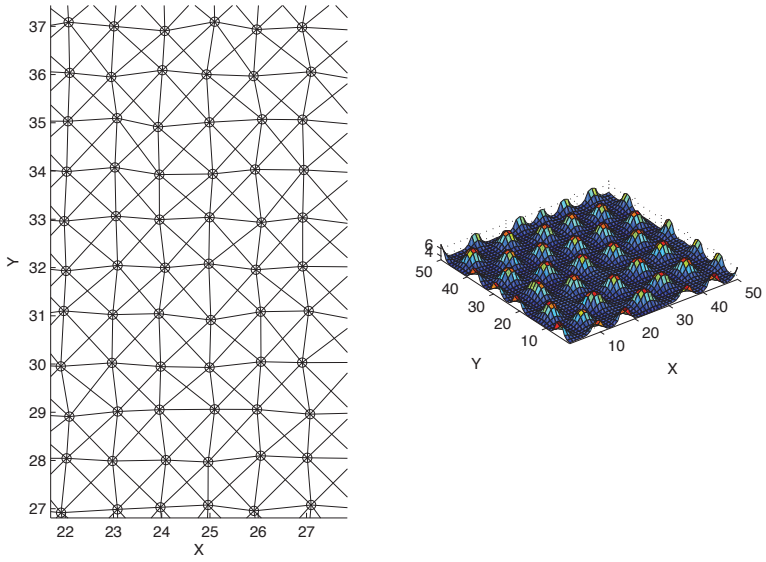

Figure 7: Turing Spot Pattern Result for 0.2 Error in Node Positions.

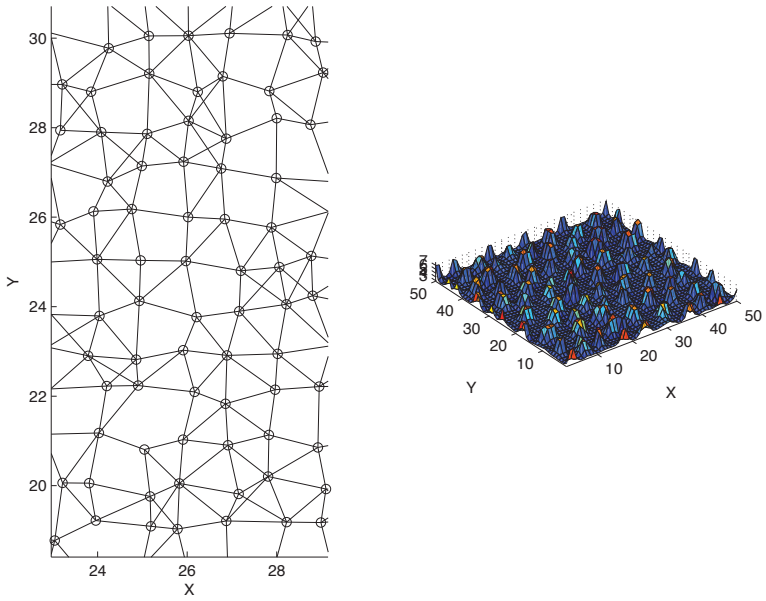

Figure 8: Turing Spot Pattern Result for 0.5 Error in Node Positions.

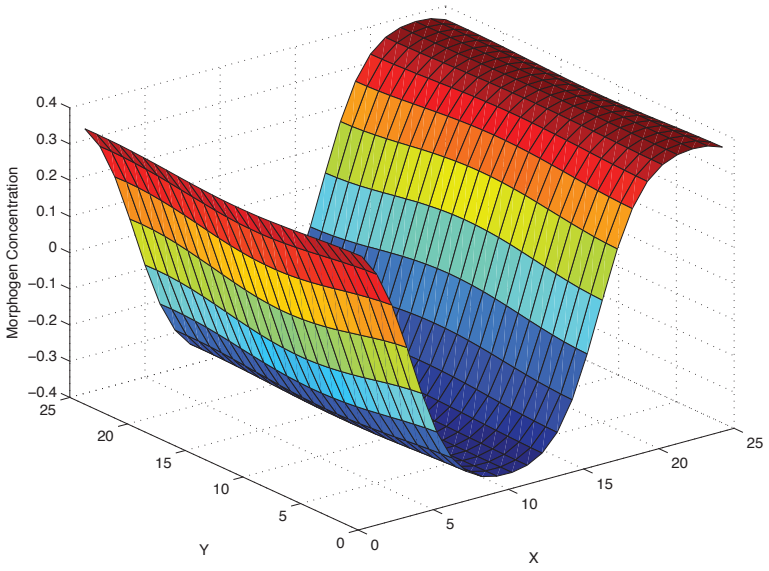

Figure 9: Ermentrout Strip Pattern Result for Wrap-around Connectivity.

size. For our work here, we assume that the diameter of the *S-Net* can be found, and from this a good estimate of the NxN size of the (displaced) grid. Figure 9 shows the result of this process; note, however, that this grid has wrap-around connectivity. Of course, wrap-around connectivity is difficult to achieve in an *S-Net*, but as shown in Figure 10, a useful result can still be obtained, although the orientation of the stripe is not aligned with either of the coördinate axes.

3 RD-Based *S-Net* Algorithms

Given the ability to form 2-D RD patterns in an *S-Net*, we now give examples of useful algorithms which exploit these patterns.

3.1 RD Leadership Protocol

It is often useful to choose a subset of the *S-Net* nodes to serve as leaders in local neighborhoods. This can be much more efficient in terms of communications, and they can also serve other roles; e.g., local coördinate frame origins (see [11] for more on this topic). *RD_LA* (Reaction-Diffusion Leadership Algorithm) is an RD-based algorithm to achieve

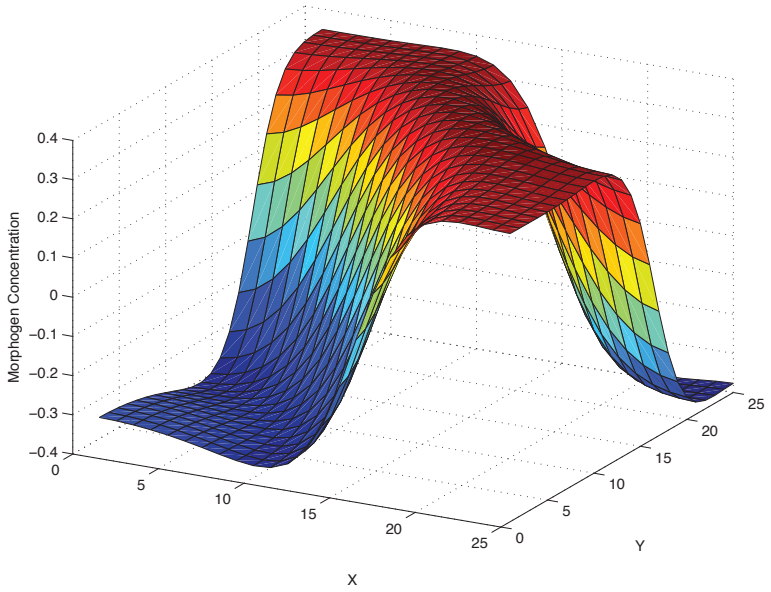

Figure 10: Ermentrout Stripe Pattern Result without Wrap-around Connectivity.

leadership selection.

Algorithm RD_LA:

1. Form RD spots.
2. For each spot, S_i
   (a) $L_i \leftarrow$ choose central node in S_i
   (b) end

Figure 11 shows a set of leader nodes produced by *RD_LA*.

3.2 Roadway Formation

One further example of the application of the spot formation reaction-diffusion process is to create straight lines in *S-Nets*. This can be done without knowing the distance between motes, and without a coördinate frame. Suppose the goal is to create stripes as shown in

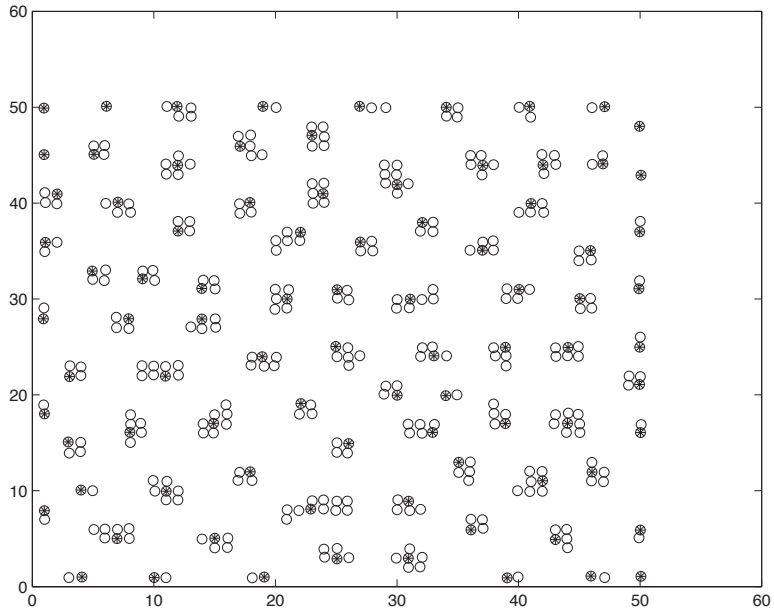

Figure 11: Leader Nodes produced by Algorithm RD_LA.

Figure 2. At each mote, determine its neighbors with lowest and highest sensor measurements. These are assumed to lie in the gradient direction. If the diffusion is restricted to take place only through these neighbors, then the spots blend in this direction and become straight lines. Figure 12 shows this result on a simulated set of motes.

4 Model Accuracy Assessment

Model Accuracy Assessment (MAA) is an important part of the modern verification and validation process [12]. This involves not only evaluation of a validation metric comparing experimental versus simulation system response quantities, but also the determination of the adequacy of the model for its intended use (see [28] for a detailed description). The incorporation of efficient and scalable probabilistic methods into model-based simultaneous state estimation and parameter identification may have a large impact on the exploitation of spatially distributed sensing and computation systems throughout a wide range of scientific domains. Spatially distributed physical phenomena such as temperature, wave propagation, etc., require observation with dynamically located sensors in order to achieve better tuned computational models and simulations. Methods developed here allow for online validation of models through direct sensor observation. Significant problems which must be overcome include the interpolation between measurement data, as well as the estimation

Figure 12: Lines produced by 2D Reaction-Diffusion Process.

of quantities which cannot be directly measured (e.g., node locations). Our major goal is to provide rigorous Bayesian Computational Sensor Networks to quantify uncertainty in (1) model-based state estimates incorporating sensor data, (2) model parameters (e.g., diffusivity coefficients), (3) sensor node model parameter values (e.g., location, bias), and input source properties (e.g., locations and extent of cracks). This is achieved in terms of extensions to our recently developed techniques (see [9, 33, 32]). We call this approach *Bayesian Computational Sensor Networks* (BCSN). These decentralized methods have low computational complexity and perform Bayesian estimation in general distributed measurement systems (i.e., sensor networks). A model of the dynamic behavior and distribution of the underlying physical phenomenon is used to obtain a continuous form from the discrete time and space samples provided by a sensor network.

Figure 13 shows the validation, calibration and prediction process as described by Oberkampf [28]. Experiments are used to establish parameters in the computational model, and these in turn affect the result of the validation metric. Both simulation experiments and physical experiments are used to help with experiment design as well as to inform the computational modeling process.

Here we use probabilistic models of macro feature properties to help select an appropriate noise model for the node placement error. Let M_a denote a node placement model which deviates from a regular grid by location error in x and y sampled from a uniform distribution $\mathcal{U}(-a, a)$. A Bayesian formulation of the probability of a given model, M_a, is:

$$P(M_a|D) = \frac{P(D|M_a)P(M_a)}{P(D)}$$

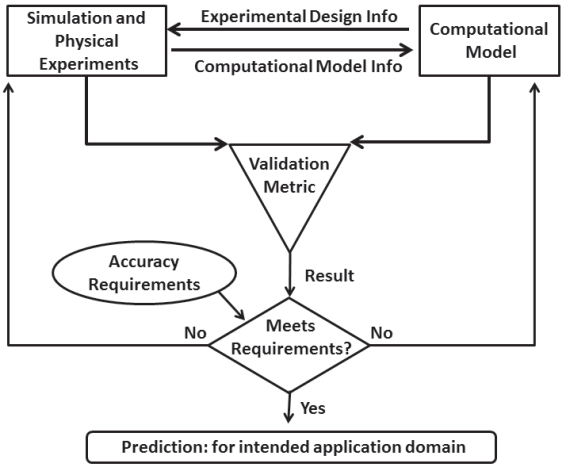

Figure 13: Model Accuracy Assessment (based on Fig. 12.4 from [28]).

where $P(M_a|D)$ is the probability of M_a given the data, D; $P(D|M_a)$ is the probability of D given M_a; $P(M_a)$ is the probability of model M_a, and $P(D)$ is the probability of the given data.

5 Simulation Experiments

We have run a set of simulation experiments to ascertain $P(D|M_a)$. We assume that $P(M_a)$ is normally distributed with mean 5 degrees, and variance 1. The number of cells is sixty, error in placement, a, is from the set $\{0, 1, 2, \ldots, 9, 10\}$, and broadcast range is 0.2. Figure 14 shows the expected number of stripes for sixty cells for the various values of error in placement and broadcast range. We ran 1100 simulations (11 angle error settings by 100 trials each) to estimate $P(D|M_a)$. Then, on a set of 1000 random values (sampled from $P(M_a)$, we calculated the error as the magnitude of the difference in the indexes of the estimated angle error and the sample error values. The number of indexes with 0 error was 73%, with one difference in index was 22.2%, with 2 difference was 4.4% and with 3 difference was 0.4 %. Figure 15 shows the differences in the indexes found by the method (i.e., it picks an error model where the error is in the set $\{0, 1, \ldots, 9, 10\}$ degrees) and the indexes of the 1,000 test samples (sorted by magnitude so it's easier to see). If the $P(M_a)$ is a sampled from a normal distribution with 7 degree mean, then 99.8% of the trial values are within one index of the actual; for mean 6, 99.9% are with 2 indexes.

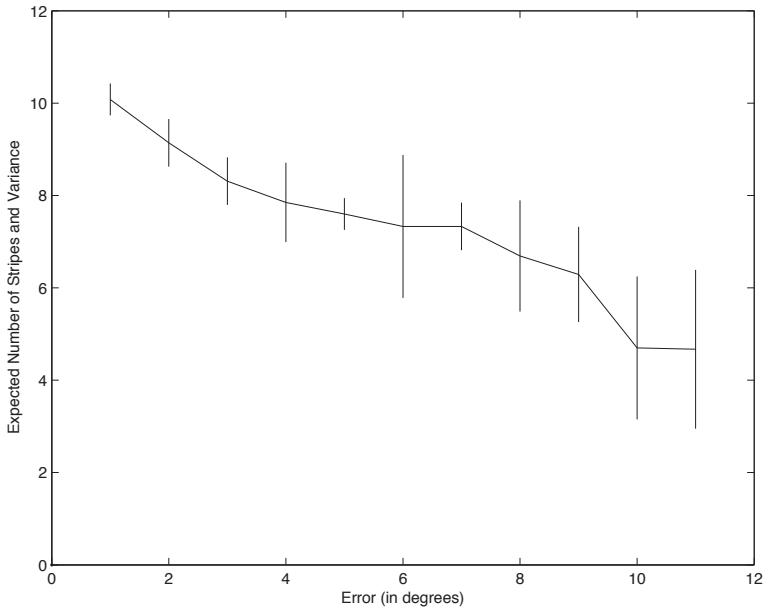

Figure 14: Expected Number of Stripes Formed vs. Error in Angle in Degrees.

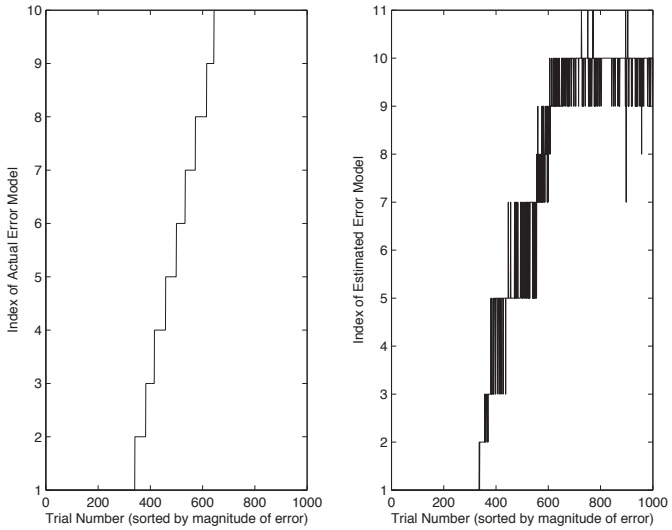

Figure 15: Comparison of Indexes into Error Models vs. Actual Indexes.

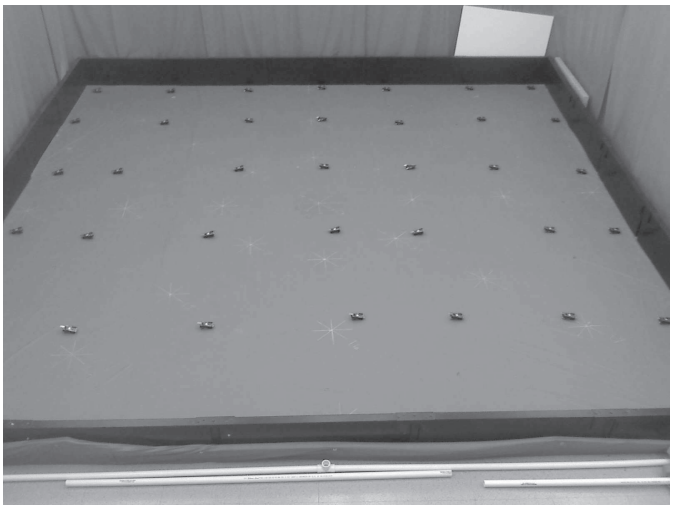

Figure 16: Layout of a set of 35 X-Bow T-Mote Sky.

6 Physical Experiments

Figure 16 shows the layout of a set of 35 X-Bow T-Mote Sky; with the small number of motes, the reaction-diffusion process leads to the formation of spots (i.e., the morphogen concentration $a > 5$). In one instance, a spot appeared after 1,250 iterations (see Figure 17); however, the spot pattern is not stable, and eventually disappears if allowed to continue. We believe that several issues are at play: the number of nodes, the asynchronous nature of the mote transmissions, as well as the locality and bi-directionality of the connectivity.

7 Conclusions and Future Work

We have described techniques for forming patterns in sensor networks based on coördinate-free reaction-diffusion systems. Such methods may be used to process data, although that is not discussed here, and to carry sensed signal information. The formation of patterns in irregular meshes has been studied here, with practical algorithms given for the computation of useful *S-Net* structures. A Bayesian model accuracy assessment method has been proposed to characterize the validity of the grid model. Finally, both simuation and physical experiments have been run to validate the models.

The next focus of our work is on the production of patterns based on sense data analysis (e.g., camouflage synthesis). Such methods may also find application in sensor network

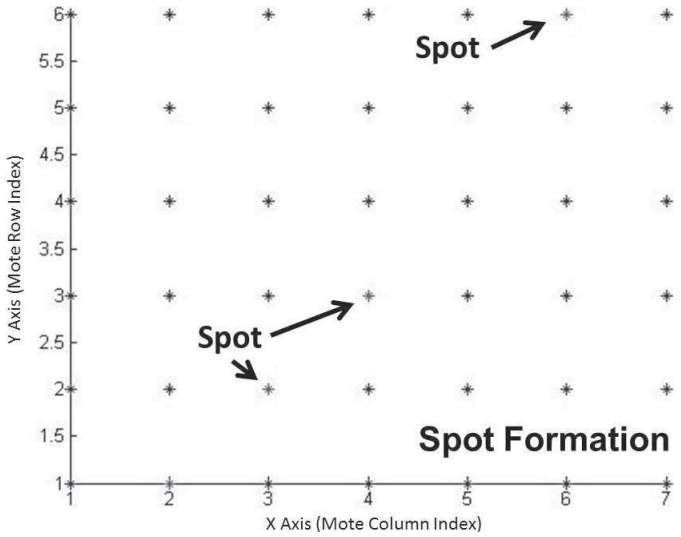

Figure 17: RD Spot Formation on a set of 42 X-Bow T-Mote Sky Devices.

security; in this scenario, a deformed pattern will emerge from a distributed computation if there are any nodes which have fallen victim to attack, or if external nodes have managed to get themselves incorporated into the *S-Net*. Of course, resource allocation and exploitation may also be based on patterns, and given the random nature of the patterns, may help conserve resources (e.g., energy) overall.

We are also exploring mesh generation in *S-Nets*. As was pointed out by Adamatzky et al. [1], physical reaction-diffusion computers can calculate Voronoi graphs. Thus, a basis exists in the reaction-diffusion computation to produce good triangulations for mote connectivity. Triangles are also important for computations on irregular meshes; e.g., for finite element methods. We are exploring this in the context of a larger set of motes.

Another area of research is the calculation of level sets [34] in the *S-Net*. These can be used for shortest path computation where an arbitrary speed function may be defined. We have shown how mobile robots can use this approach to find the lowest time path to traverse variable speed terrain [5]. However, the Eikonal equation used there may be set up as a reaction-diffusion system, and piggy-backed on the approach defined here.

Finally, stripes and spots may be of use for various purposes by mobile agents or the *S-Net*, but a more direct combination of the *S-Net* as both a sensing and display device is to be found in the creation of active camouflage. Consider the truck shown in Figure 18. Although it has a standard camouflage tarpaulin, it does not blend well with the forest behind it. Several problems exist with coloration and blobs versus stripes (e.g., tree trunks and branches), leaf texture, etc.

Figure 18: A Camouflaged Truck in the Forest.

One approach to overcome this mismatch is to pair a modeling process of the natural scene behind the truck with a display synthesis component in front of the truck. The technical basis for such a mechanism can be found in the work of Zhu and Mumford [36]. They propose (1) a theory for discovering the statistics of a set of natural images, and (2) a framework which allows the definition of reaction-diffusion equations to produce similar natural images, and in particular, they show how to remove conspicuously dissimilar segments from a scene. Specifically, they show that given a learned set of prior models that reproduce the observed statistics, the potentials of the resulting Gibbs distributions have potentials of the form:

$$U(I;\Lambda,S) = \sum_{\alpha=1}^{K} \sum_{x,y} \lambda^{\alpha}((F^{(\alpha)} \times I)(x,y))$$

where $S = \{F^{(1)}, F^{(2)}, \ldots, F^{(K)}\}$ is a set of filters and $\Lambda = \{\lambda^{(1)}, \lambda^{(2)}, \ldots, \lambda^{(K)}\}$ is the set of potential functions.

Reaction-diffusion equations are found as the gradient descent partial differential equations on $U(I;\Lambda,S)$; diffusion arises from the energy terms while pattern formation reactions are related to the inverted energy terms. These are then used to remove clutter in a scene and to denoise images. One example of this process given by Zhu and Mumford is shown in Figure 19. We propose that the resulting images can be displayed by LEDs distributed throughout the material of the camouflage canvas, and based upon our previous work in e-textiles [18, 19, 24], we believe that technical solutions exist for the realization of this goal.

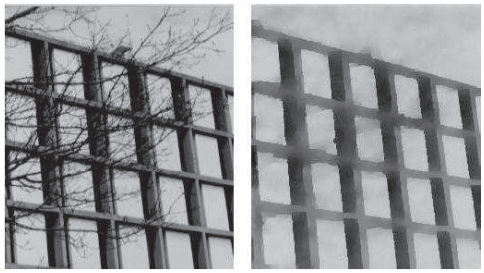

Figure 19: Zhu and Mumford [36] Clutter Removal Example.

8 Acknowledgements

This research was supported in part by AFOSR-FA9550-12-1-0291.

References

[1] A. Adamatzky, B. De Lacy Costello, and T. Asai. *Reaction-Diffusion Computers*. Elsevier, Amsterdam, The Netherlands, 2005.

[2] A. Babloyantz and J. Hiernaux. Models for cell differentiation and generation of polarity in diffusion-governed morphogenetic fields. *Bulletin of Mathematical Biology*, 37:637–657, 1975.

[3] J. Bard and I. Lauder. How Well does Turing's Theory of Morphogenesis Work? *Jnl Theor Biology*, 45:501–531, 1974.

[4] Yu Chen. Snets: Smart sensor networks. Master's thesis, University of Utah, Salt Lake City, Utah, December 2000.

[5] Yu Chen. Snets: Smart sensor networks. Master's thesis, University of Utah, Salt Lake City, Utah, December 2000.

[6] B. Ermentrout. Stripes or Spots? Nonlinear Effects in Bifurcation of Reaction-Diffusion Equations on the Square. *Proceedings: Mathematical and Physical Sciences*, 434(1891):413–417, 1991.

[7] Dario Floreano, Jean-Daniel Nicoud, and Francesco Mondada, editors. *Advances in Artificial Life, 5th European Conference, ECAL'99, Lausanne, Switzerland, September 13-17, 1999, Proceedings*, volume 1674 of *Lecture Notes in Computer Science*. Springer, 1999.

[8] M.I. Granero, A. Porati, and D. Zanacca. A bifurcation analysis of pattern formation in a diffusion goverened morphogenetic field. *Jnl of Mathematical Biology*, 4:21–27, 1977.

[9] T.C. Henderson. *Computational Sensor Networks*. Springer-Verlag, Berlin, Germany, 2009.

[10] T.C. Henderson, K. Luthy, and E. Grant. Pattern Formation in Wireless Sensor Networks. Uucs-08-008, University of Utah, Salt Lake City, UT, August 2008.

[11] Thomas C. Henderson. Leadership protocol for s-nets. In *Proc Multisensor Fusion and Integration*, pages 289–292, Baden-Baden, Germany, August 2001.

[12] Thomas C. Henderson and Narong Boonsirisumpun. Issues Related to Parameter Estimation in Model Accuracy Assessment. In *Workshop on Dynamic Data Driven Analysis Systems*, Barcelona, Spain, June 2013.

[13] Thomas C. Henderson, Mohamed Dekhil, Scott Morris, Yu Chen, and William B. Thompson. Smart sensor snow. *IEEE Conference on Intelligent Robots and Intelligent Systems*, pages 1377–1382, October 1998.

[14] Thomas C. Henderson, Jong-Chul Park, Nate Smith, and Richard Wright. From motes to java stamps: Smart sensor network testbeds. In *Proc International Conf on Intelligent Robots and Systems*, page to appear, Las Vegas, NV, October 2003.

[15] Thomas C. Henderson, Ramya Venkataraman, and Gyounghwa Choikim. Reaction-diffusion patterns in smart sensor networks. In *Proc International Conference on Robotics and Automation*, New Orleans, April 2004.

[16] C. Intanagonwiwat, R. Govindan, and D. Estrin. Directed diffusion: A scalable and robust communication paradigm for sensor networks. In *Proc. of Mobicom 2000*, Boston, August 2000.

[17] E.W. Justh and P.S. Krishnaprasad. Pattern-forming systems for control of large arrays of actuators. *Jnl of Nonlinear Sci*, 11(4):239–277, 2001.

[18] T. Kang, C.R. Merritt, B. Karaguzel, J.M. Wilson, P.D. Franzon, B. Pourdeyhimi, E. Grant, and T. Nagle. Sensors on Textile Substrates for Home-Based Healthcare Monitoring. In *Conference on Distributed Diagnosis and Healthcare (D2H2)*, pages 5–7, Arlington, VA, April 2006.

[19] B. Karaguzel, C.R. Merritt, T.H. Kang, J. Wilson, P. Franzon, H.T. Nagle, E. Grant, and B. Pourdeyhimi. Using conductive inks and non-woven textiles for wearable computing. In *Proceedings of the 2005 Textile Institute World Conference*, Raleigh, NC, March 2005.

[20] J. Koenderink. The structure of images. *Biol. Cyber.*, 50:363–370, 1984.

[21] T.C. Lacalli and L.G. Harrison. Turing's conditions and the analysis of morphogenetic models. *Jnl of Theoretical Biology*, 76:419–436, 1979.

[22] PK Maini and HG Othmer. *Mathematical Models for Biological Pattern Formation*. Springer-Verlag, Berlin, 2001.

[23] H. Meinhardt. *Models of Biological Pattern Formation*. Academic Press, London, 1982.

[24] C.R. Merritt, B. Karaguzel, T.H. Kang, J. Wilson, P. Franzon, H.T. Nagle, B. Pourdeyhimi, and E. Grant. Electrical characterization of transmission lines on specific nonwoven textile substrates. In *Proceedings of the 2005 Textile Institute World Conference*, Raleigh, NC, March 2005.

[25] J. Murray. *Mathematical Biology*. Springer-Verlag, Berlin, 1993.

[26] R Nagpal. Programmable pattern-formation and scale-independence. In *Proc International Confernce on Complex Systems (ICCS)*, Nashua, NH, June 2002.

[27] Gregoire Nicolis and Ilya Prigogine. *Exploring complexity: an Introduction*. W.H. Freeman and Co, New York, NY, 1989.

[28] W.L. Oberkampf and C.J. Roy. *Verification and Validation in Scientific Computing*. Cambridge University Press, Cambridge, UK, 2010.

[29] P. Perona, T. Shiota, and J. Malik. Anisotropic diffusion. In B. Romeny, editor, *Geometry-Driven Diffusion in Computer Vision*. Kluwer, 1994.

[30] Ilya Prigogine. *Thermodynamics of Irreversible Processes*. Interscience Publishers, New York, NY, 1968.

[31] Ilya Prigogine. *From Being to Becoming: Time and Complexity in the Physical Sciences*. W.H. Freeman and Co, San Francisco, CA, 1980.

[32] F. Sawo. *Nonlinear State and Parameter Estimation of Spatially Distributed Systems*. PhD thesis, University of Karlsruhe, January 2009.

[33] F. Sawo, T.C. Henderson, C. Sikorski, and U.D. Hanebeck. Sensor Node Localization Methods based on Local Observations of Distributed Natural Phenomena. In *Proceedings of the 2008 IEEE International Conference on Multisensor Fusion and Integration for Intelligent Systems (MFI 2008)*, Seoul, Republic of Korea, August 2008.

[34] J. A. Sethian. *Level Set Methods*. Cambridge University Press, New York, 1996.

[35] Alan Turing. The chemical basis of morphogenesis. *Philosophical Transactions of the Royal Society of London*, B237:37–72, 1952.

[36] Song Chun Zhu and David Mumford. Prior learning and gibbs reaction-diffusion. *IEEE-T on Pattern Analysis and Machine Intelligence*, 19(11):1236–1250, 1997.